Biol. Chem., Vol. 384, pp. 1411 – 1419, October/November 2003

Minireview

Ribosomal Tolerance and Peptide Bond Formation

Ada Yonath

Department of Structural Biology, The Weizmann Institute, 76100 Rehovot, Israel, and
Max-Planck-Research Unit for Ribosomal Structure, D-22603 Hamburg, Germany

In the ribosome, the decoding and peptide bond formation sites are composed entirely of ribosomal RNA, thus confirming that the ribosome is a ribozyme. Precise alignment of the aminoacylated and peptidyl tRNA 3'-ends, which is the major enzymatic contribution of the ribosome, is dominated by remote interactions of the tRNA double helical acceptor stem with the distant rims of the peptidyl transferase center. An elaborate architecture and a sizable symmetry-related region within the otherwise asymmetric ribosome guide the A→P passage of the tRNA 3'-end by a spiral rotatory motion, and ensures its outcome: stereochemistry suitable for peptide bond formation and geometry facilitating the entrance of newly formed proteins into their exit tunnel.

Key words: Peptide bond formation / Ribosomes / Translocation.

Introduction

The ribosome is the main player in the machinery translating the genetic code into proteins. This giant enzyme is a riboprotein assembly consisting of two subunits of unequal size that associate upon the initiation of protein biosynthesis. Each of the ribosomal subunits performs defined tasks. The small subunit (called 30S in prokaryotes) has key roles in the initiation of the translation process, in choosing the translated frame, decoding the genetic message, and controlling the fidelity of codon-anticodon interactions. The large subunit (called 50S in prokaryotes) catalyzes the formation of the peptide bond, channels the nascent proteins into their exit tunnel, and guides their progression through it.

An mRNA chain and three tRNA molecules interact with the ribosomes throughout the synthesis of the nascent proteins. The tRNA molecules are either aminoacylated (A-tRNA), bound to the peptidyl chain (P-tRNA), or at their free state while exiting the ribosome (E-tRNA). The mRNA chain and the anticodon loops of the tRNA molecules interact with the small subunit, whereas the acceptor stems and the tRNA 3'-ends interact with the large one. During the elongation cycle both ribosomal subunits act in concert, assisted by factor-dependent GTP hydrolysis, for the translocation of the mRNA chain and the tRNA molecules. Analysis of the three-dimensional structures of unbound ribosomal subunits from eubacteria (Figure 1A; Schluenzen *et al.*, 2000; Wimberly *et al.*, 2000; Harms *et al.*, 2001) and archaea (Ban *et al.*, 2000) as well as of the entire ribosome (Yusupov *et al.*, 2001) clearly showed that the centers of the major ribosomal activities, *i.e.* the decoding site in the small subunit and the peptide bond formation site in the large one, consist exclusively of ribosomal RNA (rRNA) (Ban *et al.*, 2000; Nissen *et al.*, 2000; Schluenzen *et al.*, 2000; Wimberly *et al.*, 2000; Harms *et al.*, 2001; Bashan *et al.*, 2003a). Hence, the primary actor in the main ribosomal functions is the rRNA, while ribosomal proteins may assist secondary activities, such as GTP hydrolysis and nascent proteins gating.

Comparative studies revealed that ribosomal components of different sizes possess inherent conformational mobility, which could be correlated with their functional tasks (Schluenzen *et al.*, 2000; Wimberly *et al.*, 2000; Yusupov *et al.*, 2001; Harms *et al.*, 2001; Pioletti *et al.*, 2001; Yonath, 2002a,b; Agmon *et al.*, 2003; Bashan *et al.*, 2003a; Berisio *et al.*, 2003a). Among the large movable domains are the head and the platform of the small subunit, the two lateral protuberances of the large subunit (Figure 1A) and several intersubunit bridges, some of which may also assist tRNA translocation (Yonath, 2002a,b; Agmon *et al.*, 2003). Of particular interest is the base of nucleotide A2602 (*E. coli* numbering system is used throughout), which was shown to have a critical role in tRNA 3'-end passage from the A- to the P-site (Agmon *et al.*, 2003; Bashan *et al.*, 2003a,b) as well as in the release of the nascent peptide during translation termination (Polacek *et al.*, 2003).

Remote Interactions and Binding Variability

The key for maintaining the ribosome in its functionally active state is the precise and accurate positioning of the intersubunit bridges. These bridges form upon subunit association from components belonging to the two subunits and may have different conformations in the associated ribosome and the free subunit. B2a is one of the major intersubunit bridges. The large ribosomal subunit portion of this bridge belongs to helix H69, which was found to be very flexible (Harms *et al.*, 2001; Yonath, 2002a,b), thus readily disordered (Ban *et al.*, 2000).

Based on the interactions made by Helix H69, it seems that the ribosome benefits from its flexibility beyond

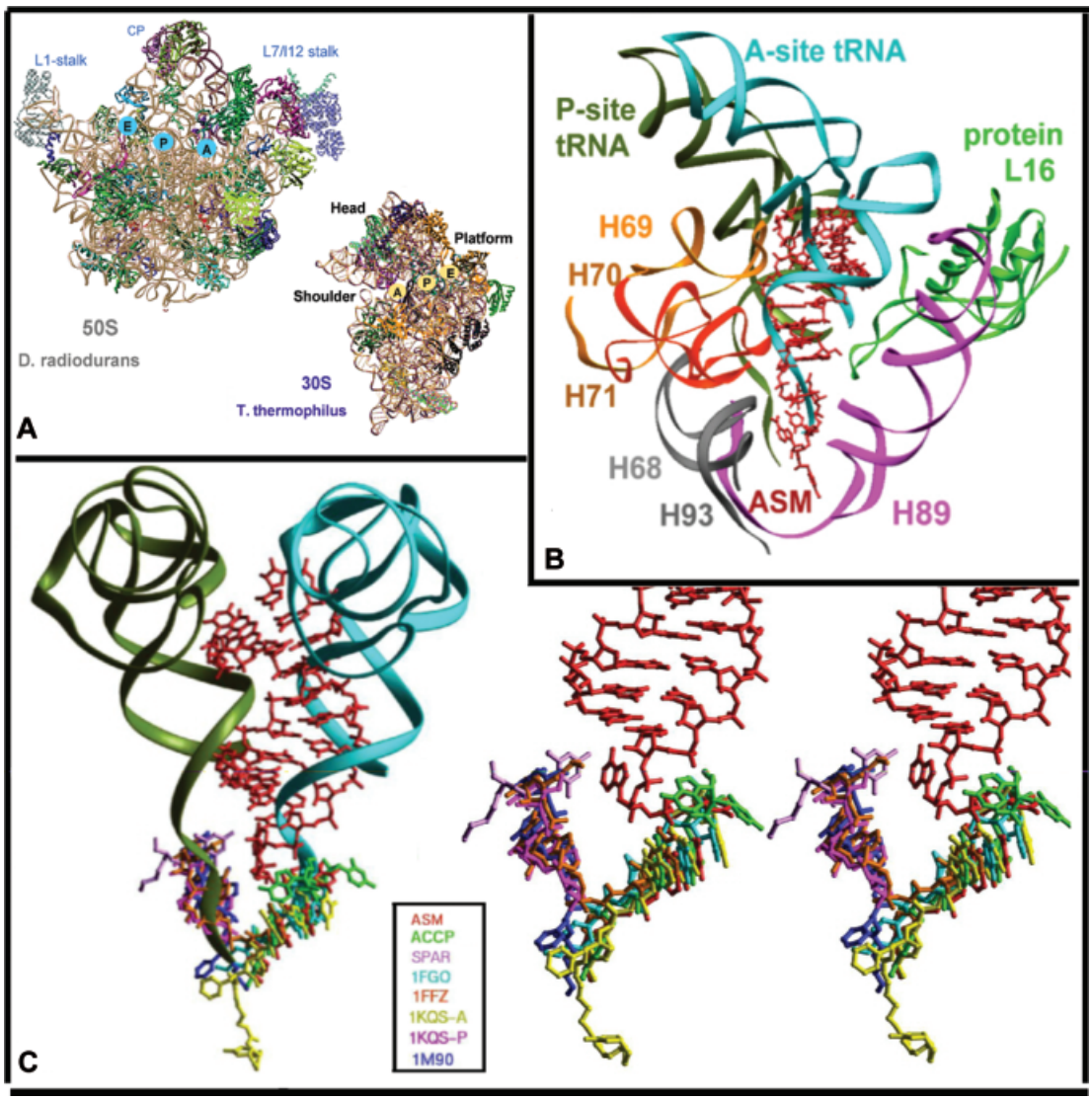

Fig. 1 The Peptidyl Transferase Center (PTC).
(A) The front views, *i.e*. the subunit interfaces, of the two eubacterial ribosomal subunits, as determined by us (Schluenzen *et al.*, 2000; Harms *et al.*, 2001). The backbone of the ribosomal RNA is shown in brown and the proteins are colored arbitrarily. The ribosomal features related to the text are depicted. A, P, and E designate the approximate position where anticodon loops and the elbows of the three tRNA molecules interact with the small and the large ribosomal subunits, respectively.
(B) A view of the PTC and its environment in D50S, together with the substrate analog, ASM, and docked A- and P-site tRNAs, according to Yusupov *et al.* (2001).
(C) Left: superposition of the locations of several bound analogs on the positions of ASM and the docked tRNAs. Right: a stereo view of the lower part of the Figure shown on the left side. The color code for all compounds is shown in the insert. D50S-bound compounds are called ASM, ACCP (a tetranucleotide composed of ACC bound to puromycin) and SPAR (sparsomycin bound to D50S). The PDB accession codes are shown for the compounds bound to H50S. Among those 1KQS-A and 1KQS-P are the A-site and P-site bound analogs, extracted from the 1KQS united file.

bridging. Helix 69 and its extension, H70, originate near the peptidyl transferase center (PTC) and stretch toward the decoding site in the small subunit. Connecting the two ribosomal active sites, this bridge seems to be a possible candidate for the transmission of signals between them. In addition, its proximity to both the A- and the P-site tRNAs suggests its participation in translocation, presumably by acting as a 'crane' that assists factor-triggered translocation of the tRNA acceptor stems, consistent with earlier suggestions (Dabrowski *et al.*, 1998; Polacek *et al.*, 2000). This multi-task ribosomal feature is also a constituent of the PTC wall (Figure 1B) and as such it was found to be instrumental for accurate positioning of the A-site tRNA (Agmon *et al.*, 2003; Bashan *et al.*, 2003a,b).

The relative significance of the interactions of various tRNA regions with the ribosome were assessed by exploiting complexes of the large ribosomal subunit from

Deinococcus radiodurans (D50S) with substrate analogs, designed to mimic different tRNA regions. The sizes of these mimics ranged from aminoacylated tetra-nucleotides, called ACCP, to oligomers of up to 35 nucleotides corresponding to the entire tRNA acceptor stem and its aminoacylated 3'-end (called ASM). Analysis of the binding modes of these mimics showed clearly that precise positioning of the aminoacylated tRNA 3'-end is governed by remote interactions of the helical regions of the acceptor stem with the upper side of the PTC (Figure 1B), primarily with protein L16 and helix H69 (Agmon *et al.*, 2003; Bashan *et al.*, 2003a). These remote interactions cannot be formed by short substrate analogs, such as ACCP. They are also missing when the interacting ribosomal components are disordered, as is the case of the crystal structure of large ribosomal subunit from

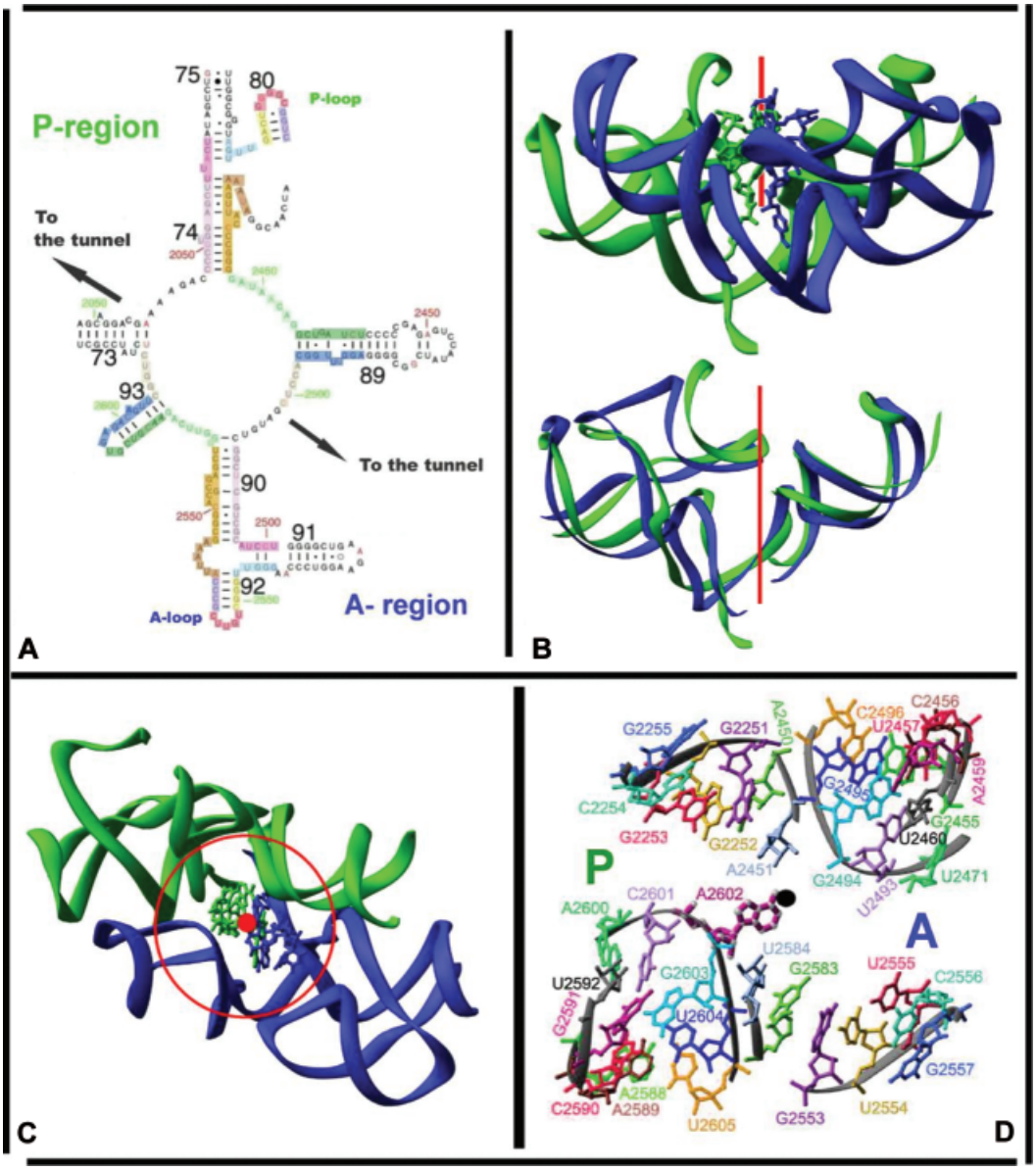

Fig. 2 The Symmetry-Related Region.
(A) Two dimensional diagram of a portion of the 23S RNA belonging to the symmetry-related region. The imaginary line combining the two arrows pointing 'to the tunnel' represent the border between the two symmetry-related regions. Symmetry-related features are colored identically.
(B-D) Ribbon representations of the backbone of the symmetry-related region. Components belonging to the A-region (below the imaginary line described in panel A) are colored blue, and to the P-site region are green. The symmetry axis is shown in red. The A-site aminoacylated 3'-end is shown in blue, and its derived P-site in green.
(B) Top: a view perpendicular to the two-fold symmetry axis. Bottom: superposition of the two symmetry-related regions.
(C) A view down the axis. The red circle shows the approximate border of the inner part of the symmetry related region shown in (D).
(D) A detailed view of the inner part shown in (D). Symmetry-related bases are colored identically.

Haloarcula marismortui, H50S (Ban *et al.*, 2000), even when a tRNA mimic is bound that is, in principle, sufficiently long (Nissen *et al.*, 2000). In the absence of the remote interactions each of the tRNA mimics binds to the PTC in a similar, albeit distinctly different mode, and only occasionally their binding modes is close to that of the remotely interacting mimics (Figure 1C).

Careful analysis of all ligands of H50S (Moore and Steitz, 2003) and D50S (Bashan *et al.*, 2003) lacking remote interactions indicated that common to these binding modes is the requirement for conformational rearrangements in order to participate in peptide bond formation. These rearrangements may involve movements of the analogs as well as alterations in the PTC conformation. Such conformational adjustments are bound to consume time, thus rationalizing the relatively slow peptidyl bond formation by short puromycin derivatives (Moore and Steitz, 2003). Support for the latter suggestion is the variability in PTC conformations, observed despite its high sequence conservation, and proposed to be correlated to the functional state of the ribosomal particle (Yusupov *et al.*, 2001; Yonath, 2002a,b). Importantly, a Watson-Crick base pair between G2553 in the PTC A-region and the nucleotide mimic corresponding to tRNA C75, identified previously by biochemical methods (Kim and Green, 1999), appears to be a common feature in all D50S and H50S complexes, regardless of their exact orientation.

A Symmetry-Related Region within a Giant Asymmetric Particle

Somewhat unexpectedly, despite the asymmetric nature of the ribosome, a symmetry-related region of significant size, containing about two hundred nucleotides (Figure 2A–C), was revealed in all known structures of the large ribosomal subunit (Ban *et al.*, 2000; Nissen *et al.*, 2000; Schluenzen *et al.*, 2001; Harms *et al.*, 2001; Yusupov *et al.*, 2001; Schmeing *et al.*, 2002; Hansen *et al.*, 2002a,b; Bashan *et al.*, 2003a; Berisio *et al.*, 2003a,b; Schluenzen *et al.*, 2003). The requirement to host within the PTC the A- and the P-site tRNA 3'-ends, which are almost identical chemically, in an orientation suitable for peptide bond formation, imply similar interactions with the PTC, hence justifying the existence of a symmetry-related region. The detection of the same symmetry relation even in complexes of H50S with partially disordered substrate analogs and inaccurate intermediates (Nissen *et al.*, 2000; Moore and Steitz, 2003) indicates the functional relevance of the ribosome internal symmetry.

A two-fold rotation axis was identified in the middle of the symmetry-related region (Figure 2B–D) in close proximity to nucleotide A2602 (Figure 2D). In the complex of D50S-ASM this axis coincides with the P-O3' bond connecting the tRNA double helical features with its single-stranded 3'-end, the moiety carrying the amino acids. This overlap is suggestive of a sovereign rotatory motion of the A-site tRNA 3'-end through the PTC pocket, an arched void of a width sufficient to accommodate tRNA 3'-ends. Analysis of the PTC architecture indicated that the PTC wall that is located farthest away from the subunit interface, called the rear wall (Agmon *et al.*, 2003; Bashan *et al.*, 2003a,b), forms a scaffold that guides the rotary motion of the 3'-tRNA. Two nucleotides, A2602 and U2585, that bulge into the PTC center and do not obey the two-fold symmetry, seem to provide a double-anchor for this motion at the PTC front side (Figure 3A). The rear wall and front anchor nucleotides involved in this guidance also confine the precise path for the rotating moiety.

A2602 displays striking conformational diversity (Figure 3B). Superposition of all its known conformations showed that it can undergo a flip of about 180° (Agmon *et al.*, 2003; Bashan *et al.*, 2003a,b). The high variability of its conformations suggests that it plays a dynamic role in the passage of the tRNA 3'-end from the A- to the P-site, and that its conformational changes may be synchronized with the rotatory motion. Hence, A2602 was proposed to act as a conformational switch within the PTC, propelling the 3'-end-rotating moiety, presumably in concert with the action of helix H69, the feature assisting the translocation near the subunit interface.

This internal two-fold symmetry relates to the backbone fold and the nucleotide centers-of-mass. It is maintained despite the PTC conformational mobility and the variability. Superposition of all known structures of free and of liganded large subunits indicate a similar backbone fold, whereas noticeable conformational changes were detected in the orientations of several nucleotides (Figure 4A–C). Some of these differences cause local deviations from the two-fold symmetry, but do not influence its overall appearance.

The Rotatory Motion and Peptide Bond Formation

The coincidence of the two-fold symmetry axis with the bond connecting the tRNA 3'-end with its helical regions implies two independent movements within the tRNA acceptor stem: a spiral two-fold rotation of the A-site tRNA 3'-end within the PTC, and a shift of the tRNA acceptor stem, as an integral part of the overall tRNA translocation, regardless of its fashion (Rheinberger *et al.*, 1981; Lill and Wintermeyer, 1987; Moazed and Noller, 1989; Noller *et al.*, 2002).

The most significant biological implication of the two-fold rotation is the creation of a favorable stereochemistry for peptide bond formation with no significant conformational rearrangements (Figure 3C). For properly positioned substrates, the guidance provided to the rotatory motion by the PTC nucleotides leads to an orientation and a distance suitable for a nucleophilic attack of the A-site primary amine on the P-site tRNA carbonyl carbon. Such attack should readily occur at pH 7.2-8, found to be optimal for protein biosynthesis in many organisms, including *E. coli* and *H. marismortui* (Miskin *et al.*, 1968; Saruyama and Nierhaus, 1985; Shevack *et al.*, 1985; Bartetzko and Nierhaus, 1988; Moazed and Noller, 1989; Rodriguez-

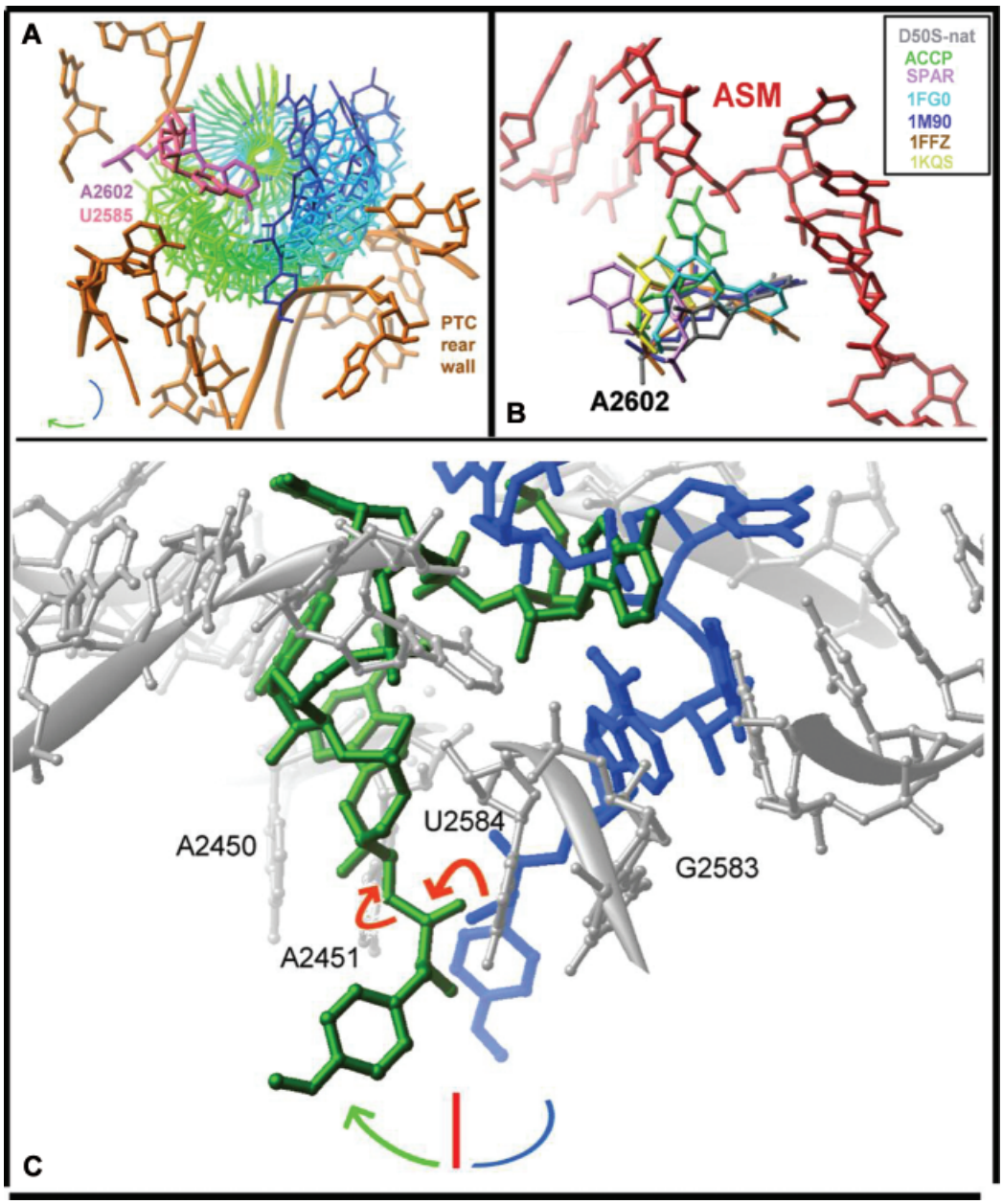

Fig. 3 The Rotary Motion and Its Linkage to Peptide Bond Formation.
(A) The A- to P-site passage rotatory motion. The blue-green arrow symbolizes the direction of the rotatory motion around the two-fold axis, with the 3'-end of ASM as the rotating moiety. Snapshots, 15 degrees apart, are shown, with their color gradually changing from blue (A-site) to green (P-site). Ribosomal components are shown in gold, pink and magenta.
(B) The orientations of A2602 in several complexes are shown together with ASM. The color code is given in the insert.
(C) The proposed mechanism of peptide bond formation and of the A- to P-translocation of tRNA 3'-ends. The red arrows designate the path taken by the hydrogens, the red stick symbolizes the direction of the two-fold axis and the blue-green arrow the rotatory motion.

Fonseca *et al.*, 2000; Bayfield *et al.*, 2001). Since the pH in D50S crystals lies within this range (Harms *et al.*, 2001), the PTC conformation seen in D50S appears to reflect the conformation required for peptide bond formation, hence providing a reliable tool for illuminating the mechanism of this reaction.

The nucleophilic attack generates a tetrahedral oxyanion intermediate. The surrounding solvent can stabilize this intermediate and mediate the transfer of a hydrogen atom from the A-site tRNA α-amino group to the P-site tRNA leaving group. Reorganization from the sp^3 to sp^2 electronic state follows, and the replacement of the P-site tRNA 3'-end by the rotating moiety assists the release of the leaving group, thus triggering translocation (Figure 3C). Thus, the A- to P-site passage seems to be synchronized with peptide-bond formation, or triggered

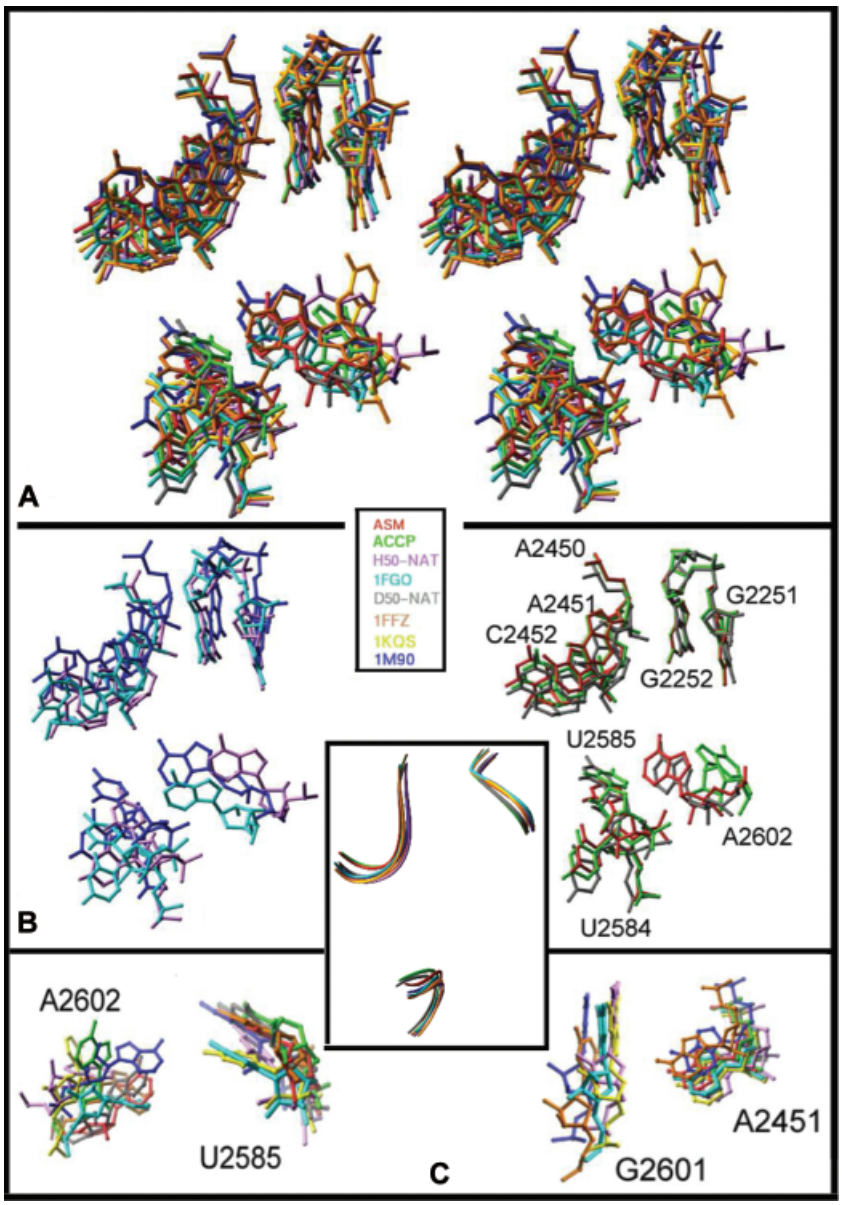

Fig. 4 Superpositions of Selected Regions of the PTC, Demonstrating Its Variability.
The insert shows the rRNA backbone. The nucleotide positions are identical in all views, and their numbers are marked on the right of panel (B). The structure sources, shown in the insert, are either named (as in Figure 1) or indicated by the PDB number.
(A) A stereo view of the superposition of all of the structures mentioned in the insert.
(B) Mono views of selected structures. Left: complexes of H50S. Right: complexes of D50S.
(C) Detailed views of the conformations of four PTC nucleotides.

by it. Ribosomal components may, however, contribute to rate enhancement of the reaction (Katunin *et al.*, 2002).

This rotatory motion is a major component of a unified machinery, integrating peptide bond formation, translocation, and nascent protein progression. The latter task is facilitated by the spiral nature of the two-fold rotation that ensures the entrance of the nascent peptide into the ribosomal exit tunnel, shown recently to possess intrinsic conformational mobility that enables gating and discrimination (Agmon *et al.*, 2003; Berisio *et al.*, 2003a; Bashan *et al*., 2003b). The sole geometrical requirement for this mechanism is that the initial P-site tRNA has the flipped orientation. Comparison of potential interactions in the two PTC binding sites shows that, compared to the A-site, the P-site contains an extra interaction that can be exploited by a flipped tRNA 3'-end, indicating the preference for this mode of binding when both sites are available.

The detection of a two-fold symmetry in all known structures of the large subunit, the high conservation of most nucleotides belonging to the symmetry related region, the ensured entrance of nascent proteins into the tunnel, the possible mediation of signal transmissions between the incoming and the leaving tRNA molecules

by the symmetry-related region (Agmon *et al.*, 2003; Bashan *et al.*, 2003b), and the resulting mutual orientation suitable for peptide bond formation, are consistent with the universality of the proposed unified mechanism.

An Alternative Mechanism

An alternative hypothesis suggested that the ribosome's enzymatic activity resembles a reverse acylation step in the mechanism of serine proteases, with A2451 playing the same general base role as histidine-57 in chymotrypsin. According to this proposed mechanism specific PTC nucleotides participate in the actual nucleophilic attack and provide stabilization of the oxyanion intermediate (Nissen *et al.*, 2000). However, this suggestion was inferred from the crystal structure of H50S in complex with a partially disordered tRNA-mimic and a compound, presumed to be a reaction intermediate, and raised considerable doubt (Barta *et al.*, 2001; Bayfield *et al.*, 2001; Polacek *et al.*, 2001; Thompson *et al.*, 2001). These uncertainties were substantiated by crystallographic analysis of the structures of additional H50S complexes (Hansen *et al.*, 2002b; Moore and Steitz, 2003). Importantly, although the additional experiments were performed under identical conditions and with the same crystal form used in the previous studies, they led to radically different observations (Hansen *et al.*, 2002b; Moore and Steitz, 2003). Hence, it appears that parallelism between the synthesis of the peptide bond and its enzymatic hydrolysis does not apply, and that there is no indication that the creation of the peptide bond by the most intricate molecular machine resembles a reverse common enzymatic hydrolysis of this bond.

Five H50S complexes (Moore and Steitz, 2003) were needed for reaching the conclusion evident by inspecting the structure of D50S (Harms *et al.*, 2001) and verified by a single complex of it (Bashan *et al.*, 2003a). Compared to all H50S bound analogs, the D50S complex is unique (Figure 1C), since D50S crystals are capable of providing the crucial remote interactions (Figure 1B), as their helix H69 is fully ordered (Harms *et al.*, 2001). The still open question relates to the relevance of the structures of H50S complexes and their likelihood to lead to the elucidation of the mechanism of peptide bond formation. It was argued that the compounds originally used (Nissen *et al.*, 2000) presented inaccurate pictures of the reaction (Moore and Steitz, 2003) and thus led to the observed discrepancies. However, the requirement for conformational rearrangements of all binding modes observed in H50S-analog complexes, including the complex containing a tRNA mimic similar to ASM, which binds properly to D50S, challenges this reasoning. It seems, therefore, that H50S crystals provide a system that is only partially appropriate for revealing the exact mechanism for peptide bond formation.

One of the main concerns about the crystalline H50S subunits relates to the disorder of almost all of the functionally relevant features observed in the crystal structure (Ban *et al.*, 2000). This disorder seems to be linked to the deviations of the environment within the H50S crystals from the conditions required for efficient protein biosynthesis. Not only the concentration of the intra-crystals salts is about half of the required concentration (Ginzburg *et al.*, 1970; Shevack *et al.*, 1985), but also the pH is far from the optimum for protein synthesis (Moore and Steitz, 2003). Interestingly, a single peptide bond could be formed within the H50S crystals, despite these discrepancies. However, the resulting dipeptide was bound to the 3'-end of the A-site mimic, and was not passed to the P-site, although the H50S crystals posses sufficient space for such passage. This observation was ascribed to the low affinity of puromycin products to the P-site (Schmeing *et al.*, 2002; Hansen *et al.*, 2002b; Moore and Steitz, 2003), but it may also be due to the initial binding geometry that is less suitable for the rotating-moiety/rear wall interactions. This suggestion is supported by simulation studies showing that applying the rotatory motion to mimics positioned in less than optimal geometry led to collisions with the PTC rear wall or to final orientations that are less suitable for peptide bond formation. These results confirm the PTC tolerance to various binding modes, including those leading to peptide bond formation but not to chain elongation, thus showing that the mere creation of a single peptide bond may not represent the actual events that lead to a nascent proteins. They also substantiate the suggestion that precise substrate alignment is key for the processivity of peptide bond formation.

Conclusion

We found that the primary catalytic activity of the ribosome is the provision of the structural frameworks enabling accurate positioning of the tRNA substrates as well as the template that guides tRNA 3'-end translocation. Remote interactions govern the correct substrate placement, mandatory for efficient peptide bond formation. In the absence of these interactions, the PTC tolerates various binding modes, all requiring conformational rearrangements for participating in peptide bond formation. The diversity of the PTC binding modes demonstrates the relative ease of accommodating compounds resembling tRNA 3'-ends, which may or may not represent the actual stereochemistry enabling the formation of polypeptides.

Once positioned well, the A-site tRNA 3'-end can flip into the P-site by rotating around the bond connecting the single strand 3'-end to the tRNA double helical regions. In well-placed substrates this bond coincides with a two-fold rotation axis identified within a sizable symmetry-related region, a unique feature within the otherwise asymmetrical ribosome. This rotatory motion occurs in concert with peptide bond formation, directs the passage from A- to P-site and ensures the progression of the nascent protein through its exit tunnel.

Acknowledgments

Thanks are due to J.M. Lehn, M. Lahav and R. Berisio for critical discussions, to the members of the ribosome research groups at the Weizmann Institute and the Max-Planck-Society, Germany, for contributing to different stages of this work. These studies were performed and assisted by the staff of station ID19/SBC/APS/ANL and ID14/ESRF-EMBL/Grenoble, France. The Max-Planck-Society, the Kimmelman Center for Macromolecular Assembly, the US National Institutes of Health (GM34360) and the German Ministry for Science and Technology (BMBF05-641EA) provided support. The author holds the Helen and Martin Kimmel Professorial Chair.

References

Agmon, I., Auerbach, T., Baram, D., Bartels, H., Bashan, A., Berisio, R., Fucini, P., Hansen, H. A., Harms, J., Kessler, M. *et al.* (2003). On peptide bond formation, translocation, nascent protein progression and the regulatory properties of ribosomes. Eur. J. Biochem. *270*, 2543–2556.

Ban, N., Nissen, P., Hansen, J., Moore, P. B. and Steitz, T. A. (2000). The complete atomic structure of the large ribosomal subunit at 2.4 Å resolution. Science *289*, 905–920.

Barta, A., Dorner, S. and Polacek, N. (2001). Mechanism of ribosomal peptide bond formation. Science *291*, 203.

Bartetzko, A. and Nierhaus, K.H. (1988). Mg^{2+}/NH_4^+/polyamine system for polyuridine-dependent polyphenylalanine synthesis with near *in vivo* characteristics. Methods Enzymol. *164*, 650–658.

Bashan, A., Agmon, I., Zarivach, R., Schluenzen, F., Harms, J., Berisio, R., Bartels, H., Franceschi, F., Auerbach, T., Hansen, H. A. S. *et al.* (2003a). Structural basis for a unified machinery of peptide bond formation, translocation and nascent chain progression. Mol. Cell *11*, 91–102.

Bashan, A., Zarivach, R., Schluenzen, F., Agmon, I., Harms, J., Auerbach, T., Baram, D., Berisio, R., Bartels, H., Hansen, H.A.S. *et al*. (2003b). Ribosomal crystallography: peptide bond formation and its inhibition. Biopolymers *70*, 19–41.

Bayfield, M. A., Dahlberg, A. E., Schulmeister, U., Dorner, S. and Barta, A. (2001). A conformational change in the ribosomal peptidyl transferase center upon active/inactive transition. Proc. Natl. Acad. Sci. USA *98*, 10096–10101.

Berisio, R., Schluenzen, F., Harms, J., Bashan, A., Auerbach, T., Baram, D. and Yonath, A. (2003a). Structural insight into the role of the ribosomal tunnel in cellular regulation. Nature Struct. Biol. *10*, 366–370.

Berisio, R., Harms, J., Schluenzen, F., Zarivach, R., Hansen, H. A., Fucini, P. and Yonath, A. (2003b). Structural insight into the antibiotic action of telithromycin against resistant mutants. J. Bacteriol. *185*, 4276–4279.

Dabrowski, M., Spahn, C. M., Schafer, M. A., Patzke, S. and Nierhaus, K. H. (1998). Protection patterns of tRNAs do not change during ribosomal translocation. J. Biol. Chem. *273*, 32793–32800.

Ginzburg, M., Sachs, L. and Ginzburg, B. Z. (1970). Ion metabolism in a Halobacterium. I. Influence of age of culture on intracellular concentrations. J. Gen. Physiol. *55*, 187–207.

Hansen, J.L., Ippolito, J.A., Ban, N., Nissen, P., Moore, P.B. and Steitz, T. A. (2002a). The structures of four macrolide antibiotics bound to the large ribosomal subunit. Mol. Cell *10*, 117–128.

Hansen, J. L., Schmeing, T. M., Moore, P. B. and Steitz, T. A. (2002b). Structural insights into peptide bond formation. Proc. Natl. Acad. Sci. USA *99*, 11670–11675.

Harms, J., Schluenzen, F., Zarivach, R., Bashan, A., Gat, S., Agmon, I., Bartels, H., Franceschi, F. and Yonath, A. (2001). High resolution structure of the large ribosomal subunit from a mesophilic eubacterium. Cell *107*, 679–688.

Katunin, V., Muth, G., Strobel, S., Wintermeyer, W. and Rodnina, M. (2002). Important contribution to catalysis of peptide bond formation by a single ionizing group within the ribosome. Mol. Cell *10*, 339–346.

Kim, D. F. and Green, R. (1999). Base-pairing between 23S rRNA and tRNA in the ribosomal A site. Mol. Cell *4*, 859–864.

Lill, R. and Wintermeyer, W. (1987). Destabilization of codon-anticodon interaction in the ribosomal exit site. J. Mol. Biol. *196*, 137–148.

Miskin, R., Zamir, A. and Elson, D. (1968). The inactivation and reactivation of ribosomal-peptidyl transferase of *E. coli*. Biochem. Biophys. Res. Commun. *33*, 551–557.

Moazed, D. and Noller, H. F. (1989). Intermediate states in the movement of transfer RNA in the ribosome. Nature *342*, 142–148.

Moore, P. B. and Steitz, T. A. (2003). After the ribosome structures: how does peptidyl transferase work? RNA *9*, 155–159.

Nissen, P., Hansen, J., Ban, N., Moore, P. B. and Steitz, T. A. (2000). The structural basis of ribosome activity in peptide bond synthesis. Science *289*, 920–930.

Noller, H. F., Yusupov, M. M., Yusupova, G. Z., Baucom, A. and Cate, J. H. (2002). Translocation of tRNA during protein synthesis. FEBS Lett. *514*, 11–16.

Pioletti, M., Schluenzen, F., Harms, J., Zarivach, R., Gluehmann, M., Avila, H., Bashan, A., Bartels, H., Auerbach, T., Jacobi, C. *et al.* (2001). Crystal structures of complexes of the small ribosomal subunit with tetracycline, edeine and IF3. EMBO J. *20*, 1829–1839.

Polacek, N., Patzke, S., Nierhaus, K. H. and Barta, A. (2000). Periodic conformational changes in rRNA: monitoring the dynamics of translating ribosomes. Mol. Cell *6*, 159–171.

Polacek, N., Gaynor, M., Yassin, A. and Mankin, A. S. (2001). Ribosomal peptidyl transferase can withstand mutations at the putative catalytic nucleotide. Nature *411*, 498–501.

Polacek, N., Gomez, M. J., Ito, K., Xiong, L., Nakamura, Y. and Mankin, A. (2003). The critical role of the universally conserved A2602 of 23S ribosomal RNA in the release of the nascent peptide during translation termination. Mol. Cell *11*, 103–112.

Rheinberger, H. J., Sternbach, H. and Nierhaus, K. H. (1981). Three tRNA binding sites on *Escherichia coli* ribosomes. Proc. Natl. Acad. Sci. USA *78*, 5310–5314.

Rodriguez-Fonseca, C., Phan, H., Long, K. S., Porse, B. T., Kirillov, S. V., Amils, R. and Garrett, R. A. (2000). Puromycin-rRNA interaction sites at the peptidyl transferase center. RNA *6*, 744–754.

Saruyama, H. and Nierhaus, K. H. (1985). A highly efficient poly(U)-dependent poly(Phe) synthesis system for the extreme halophile archaebacterium *Halobacterium halobium*. FEBS Lett. *183*, 390–394.

Schluenzen, F., Tocilj, A., Zarivach, R., Harms, J., Gluehmann, M., Janell, D., Bashan, A., Bartels, H., Agmon, I., Franceschi, F. and Yonath, A. (2000). Structure of functionally activated small ribosomal subunit at 3.3 Å resolution. Cell *102*, 615–623.

Schluenzen, F., Zarivach, R., Harms, J., Bashan, A., Tocilj, A., Albrecht, R., Yonath, A. and Franceschi, F. (2001). Structural basis for the interaction of antibiotics with the peptidyl transferase centre in eubacteria. Nature *413*, 814–821.

Schluenzen, F., Harms, J., Franceschi, F., Hansen, H. A. S., Bartels, H., Zarivach, R. and Yonath, A. (2003). Structural basis for the antibiotic activity of ketolides and azalides. Structure *11*, 329–338.

Schmeing, T. M., Seila, A. C., Hansen, J. L., Freeborn, B., Soukup, J. K., Scaringe, S. A., Strobel, S. A., Moore, P. B. and Steitz, T. A. (2002). A pre-translocational intermediate in protein synthesis observed in crystals of enzymatically active 50S subunits. Nature Struct. Biol. *9*, 225 – 230.

Shevack, A., Gewitz, H. S., Hennemann, B., Yonath, A. and Wittmann, H. G. (1985). Characterization and crystallization of ribosomal particles from *Halobacterium marismortui*. FEBS Lett *184*, 68 – 71.

Thompson, J., Kim, D. F., O'Connor, M., Lieberman, K. R., Bayfield, M. A., Gregory, S. T., Green, R., Noller, H. F. and Dahlberg, A. E. (2001). Analysis of mutations at residues A2451 and G2447 of 23S rRNA in the peptidyltransferase active site of the 50S ribosomal subunit. Proc. Natl. Acad. Sci. USA *98*, 9002 – 9007.

Wimberly, B. T., Brodersen, D. E., Clemons, W. M., Jr., Morgan-Warren, R. J., Carter, A. P., Vonrhein, C., Hartsch, T. and Ramakrishnan, V. (2000). Structure of the 30S ribosomal subunit. Nature *407*, 327 – 339.

Yonath, A. (2002a). The search and its outcome: high-resolution structures of ribosomal particles from mesophilic, thermophilic, and halophilic bacteria at various functional states. Annu. Rev. Biophys. Biomol. Struct. *31*, 257 – 273.

Yonath, A. (2002b). High-resolution structures of large ribosomal subunits from mesophilic eubacteria and halophilic archaea at various functional states. Curr. Protein Pept. Sci. *3*, 67 – 78.

Yusupov, M. M., Yusupova, G. Z., Baucom, A., Lieberman, K., Earnest, T. N., Cate, J. H. and Noller, H. F. (2001). Crystal structure of the ribosome at 5.5 Å resolution. Science *292*, 883 – 896.